

PNNL-30870

# Analysis methods for quantifying Xe-127 samples from the UNESE project

January 2021

Christine Johnson  
Brittany Abromeit  
Thomas Alexander  
Justin Lowrey  
Emily Mace  
Michael Mayer  
Justin McIntyre

## DISCLAIMER

This report was prepared as an account of work sponsored by an agency of the United States Government. Neither the United States Government nor any agency thereof, nor Battelle Memorial Institute, nor any of their employees, **makes any warranty, express or implied, or assumes any legal liability or responsibility for the accuracy, completeness, or usefulness of any information, apparatus, product, or process disclosed, or represents that its use would not infringe privately owned rights.** Reference herein to any specific commercial product, process, or service by trade name, trademark, manufacturer, or otherwise does not necessarily constitute or imply its endorsement, recommendation, or favoring by the United States Government or any agency thereof, or Battelle Memorial Institute. The views and opinions of authors expressed herein do not necessarily state or reflect those of the United States Government or any agency thereof.

PACIFIC NORTHWEST NATIONAL LABORATORY  
*operated by*  
BATTELLE  
*for the*  
UNITED STATES DEPARTMENT OF ENERGY  
*under Contract DE-AC05-76RL01830*

Printed in the United States of America

Available to DOE and DOE contractors from  
the Office of Scientific and Technical  
Information,  
P.O. Box 62, Oak Ridge, TN 37831-0062  
[www.osti.gov](http://www.osti.gov)  
ph: (865) 576-8401  
fax: (865) 576-5728  
email: [reports@osti.gov](mailto:reports@osti.gov)

Available to the public from the National Technical Information Service  
5301 Shawnee Rd., Alexandria, VA 22312  
ph: (800) 553-NTIS (6847)  
or (703) 605-6000  
email: [info@ntis.gov](mailto:info@ntis.gov)  
Online ordering: <http://www.ntis.gov>

# **Analysis methods for quantifying Xe-127 samples from the UNESE project**

January 2021

Christine Johnson  
Brittany Abromeit  
Thomas Alexander  
Justin Lowrey  
Emily Mace  
Michael Mayer  
Justin McIntyre

Prepared for  
the U.S. Department of Energy  
under Contract DE-AC05-76RL01830

Pacific Northwest National Laboratory  
Richland, Washington 99354

## Abstract

In the Underground Nuclear Explosions Signatures Experiment (UNESE) radioactive  $^{37}\text{Ar}$  and  $^{127}\text{Xe}$  were used as tracers in subsurface migration experiments. As part of the experiment, methods were developed to quantify  $^{127}\text{Xe}$  via  $\beta$ - $\gamma$  coincidence spectroscopy. Later examination of the results highlighted a weakness of this analysis method in samples with no  $^{127}\text{Xe}$  present, so a reanalysis of samples was performed to identify those which were falsely identified as having  $^{127}\text{Xe}$  present. Ongoing work to develop a new analysis method with targeted regions of interest is also described.

Measurements were also performed to quantify the concentration of  $^{127}\text{Xe}$  and  $^{37}\text{Ar}$  which were injected as part of UNESE Phase 2. A best value for the concentration of  $^{37}\text{Ar}$  and  $^{127}\text{Xe}$  was determined and reported here for use in future analyses of the UNESE Phase 2 results.

## Summary

As part of the Underground Nuclear Explosion Signatures Experiment (UNESE), radioactive  $^{127}\text{Xe}$  was injected into two historic underground nuclear test chimneys then sampled from various points surrounding those chimneys so that observations could be made about the transport of radioxenon in the subsurface. Once samples were collected from the various sampling locations, they were brought to PNNL for processing and counting on  $\beta$ - $\gamma$  coincidence detectors. Because of its complex decay scheme, new analysis methods were developed in order to more accurately quantify the concentration of  $^{127}\text{Xe}$  from the  $\beta$ - $\gamma$  coincidence spectra collected on these systems. More recent consideration of the results derived using this method highlighted that the method was over-predicting the concentration of  $^{127}\text{Xe}$  in cases where no xenon was present in the sample. A reanalysis effort was undertaken to identify and re-quantify those samples. This effort identified many samples early in the collection period where no xenon was present in the sample, but it also highlighted the case of a borehole where xenon likely arrived sooner than originally believed. Work was also conducted to begin development of a new method to better quantify  $^{127}\text{Xe}$  in beta gamma spectra in the future.

Additionally, as part of this work replicate measurements were made of the initial xenon source that was injected as part of UNESE Phase 2. This gas was produced via neutron irradiation of  $^{126}\text{Xe}$  and  $^{36}\text{Ar}$  at the University of Texas at Austin. Small aliquots were siphoned off the main sample and shipped to PNNL where they were analyzed in proportional counters. This analysis allowed for simultaneous quantification of both the  $^{37}\text{Ar}$  and  $^{127}\text{Xe}$ .

## Acknowledgments

The authors wish to acknowledge the National Nuclear Security Administration, Defense Nuclear Nonproliferation Research and Development, and the Underground Nuclear Explosion Signatures Experiment, a multi-year research and development project sponsored by NNSA DNN R&D and collaboratively executed by Lawrence Livermore National Laboratory, Los Alamos National Laboratory, Mission Support and Test Services, Pacific Northwest National Laboratory, and Sandia National Laboratories. This work was performed by Pacific Northwest National Laboratory under award number DE-AC05-76RL01830.

## Acronyms and Abbreviations

HPGe	High-Purity Germanium
IMS	International Monitoring System
PNNL	Pacific Northwest National Laboratory
NNSS	Nevada National Security Site
ROI	Region of Interest
UNE	Underground Nuclear Explosion
UNESE	Underground Nuclear Explosion Signatures Experiment

## Contents

Abstract.....	ii
Summary .....	iii
Acknowledgments.....	iv
Acronyms and Abbreviations.....	v
1.0 Introduction .....	1
2.0 Quantification of 2018 injection gas .....	2
3.0 Initial analysis of $^{127}\text{Xe}$ in UNESE Phase 1 samples .....	3
4.0 Improved analysis of $^{127}\text{Xe}$ in UNESE Phase 1 samples.....	5
5.0 Progress on a future analysis method.....	7
5.1 Regions of Interest (ROI) .....	7
5.2 Extracting Counts.....	9
6.0 Conclusion .....	12
7.0 References.....	13
Appendix A – UNESE Phase 1 $^{37}\text{Ar}$ Results.....	A.1
Appendix B – Initial UNESE Phase 1 $^{127}\text{Xe}$ Results .....	B.3
Appendix C – Updated UNESE Phase 1 $^{127}\text{Xe}$ Results .....	C.5

## Figures

Figure 1. The $\beta - \gamma$ coincidence spectrum of a subsurface gas sample containing $^{127}\text{Xe}$ . The triangular ROI delineated by the red line highlights the region used in the initial analysis of the $\beta$ - $\gamma$ spectra (C. Johnson et al. 2019).....	3
Figure 2. $\beta$ - $\gamma$ coincidence spectrum with traditional radioxenon ROIs along with previously defined $^{127}\text{Xe}$ ROIs in purple. (Klingberg et al. 2015).....	7
Figure 3. Newly defined ROI for $^{127}\text{Xe}$ used for calibration purposes.....	9
Figure 4. $^{127}\text{Xe}$ decay scheme with $\gamma$ and $\beta$ transition probabilities (Cagniant et al. 2014a). .....	10
Figure 5. $\beta$ single and coincidence spectra taken from a $^{127}\text{Xe}$ spike. The two $\beta$ peaks of interest are labeled in <b>blue</b> . .....	10
Figure 6. $\gamma$ single and coincidence spectra taken from a $^{127}\text{Xe}$ spike. The two $\gamma$ peaks of interest are labeled in <b>blue</b> . .....	11

## Tables

Table 1. The measured $^{37}\text{Ar}$ and $^{127}\text{Xe}$ activities in sample aliquots from the UNESE Phase 2 injection gas, decay corrected to the injection date. ....	2
Table 2. After re-analysis of the individual spectra, the following samples were determined to contain no evidence of $^{127}\text{Xe}$ .....	5



Table 3 – Average channels associated with the centroid of the $\beta$ or $\gamma$ peak in $^{127}\text{Xe}$ . .....	8
Table 4 – Energy ranges for the 4 newly defined ROIs. ....	8

## 1.0 Introduction

The Underground Nuclear Explosion Signatures Experiment (UNESE) was a multi-year research and development project created to apply a broad range of research and development techniques and technologies to nuclear explosion monitoring and nuclear nonproliferation. As part of UNESE, two noble gas migration experiments were conducted at the Nevada National Security Site (NNSS) to simulate the transport of radioactive noble gases that would be created during an underground nuclear explosion (UNE). The focus of these experiments was to study the transport of gases, particularly radioactive noble gases, through a UNE produced fracture network using only natural transport mechanisms. The UNESE Phase 1 gas migration experiment was conducted at the site of the Barnwell UNE, U-20az, while UNESE Phase 2 was conducted in and around the U-12p tunnel (P-tunnel) complex with a focus on the site of the Disko Elm UNE (C. Johnson et al. 2019; Christine Johnson et al. 2020).

In both injections a mixed radioactive tracer was used that combined two radioactive noble gases,  $^{37}\text{Ar}$  and  $^{127}\text{Xe}$ . Radioactive isotopes of xenon ( $^{131\text{m}}\text{Xe}$ ,  $^{133}\text{Xe}$ ,  $^{133\text{m}}\text{Xe}$ , and  $^{135}\text{Xe}$ ) are produced in large quantities during a UNE as fission products. The longest-lived of these isotopes,  $^{131\text{m}}\text{Xe}$ , has a half-life of 11.9 days, which makes it challenging to inject sufficient quantity to be detectable over a year-long migration experiment. Instead,  $^{127}\text{Xe}$ , with a half-life of 36.4 days, was identified as a suitable surrogate tracer and used for three underground gas migration experiments at the NNSS (Olsen et al. 2016; C. Johnson et al. 2019).

In the recent literature,  $^{127}\text{Xe}$  has been investigated as a potential quality control standard for use in the International Monitoring System (IMS) (Cagniant et al. 2014; Gohla et al. 2016; Klingberg et al. 2015). It has a 36.4 day half-life, simplifying sample preparation and shipping to remote locations and as an isotope of xenon it has an identical form factor to the isotopes of interest. In the SPALAX system, which uses a high-purity germanium (HPGe) detector to perform  $\gamma$  ray emission spectrometry,  $^{127}\text{Xe}$  has been shown to be a viable quality control source (Cagniant et al. 2014; Gohla et al. 2016). Xenon-127 has also been observed in environmental air samples on next-generation beta-gamma detection systems (Ely et al. 2020).

In  $\beta$ - $\gamma$  coincidence systems,  $^{127}\text{Xe}$  becomes significantly more difficult to fully analyze. Because of the many coincidence possibilities in a  $^{127}\text{Xe}$  spectrum, deconvolving the contributions which lead to a signal in a specific region of interest (ROI) is not straightforward. Two methods of using  $^{127}\text{Xe}$  ROIs are explored in this report and one is used to analyze samples collected during the UNESE transport experiments.

## 2.0 Quantification of 2018 injection gas

As part of UNESE Phase 2, two radioactive tracers ( $^{37}\text{Ar}$  and  $^{127}\text{Xe}$ ) were injected into the chimney of the Disko Elm UNE along with stable gas tracers. Estimates of the injected activity were made at the University of Texas at Austin when the tracers were produced and shipped but for improved subsurface transport models a more accurate knowledge of the injected activity was needed. Three aliquots of the injection gas were collected prior to shipment of the gas to the NNSS and were sent to PNNL for analysis.

The analysis method was similar to that described in (Mace et al. 2018). A small spike of gas was taken from each aliquot using volumetric expansion into an evacuated reference volume. The spikes were then mixed with P10 gas and each loaded into two proportional counters with volumes of 100 cc and 250 cc. The samples were then counted in the 0-15 keV range for between 7 and 180 minutes, detector dependent.

A double gaussian analysis was used to calculate the peak area and uncertainty for both  $^{37}\text{Ar}$  and  $^{127}\text{Xe}$  in two of the samples. Challenges with the volumetric expansion prevented full analysis of the third sample. Geometry-specific efficiencies were calculated for each of the detectors. From these measurements the activity concentration of  $^{37}\text{Ar}$  and  $^{127}\text{Xe}$  can then be determined by dividing the peak areas by the appropriate branching ratio and volume and decay-correcting the samples back to the date of the injection. The measured concentrations for two of the samples are shown in Table 1. From these measurements a best value for the activity concentration injected in the UNESE Phase 2 noble gas migration experiment was found to be  $2.64 \times 10^{13} \pm 3.83\%$  Bq/m<sup>3</sup> for  $^{37}\text{Ar}$  and  $4.98 \times 10^{13} \pm 4.47\%$  Bq/m<sup>3</sup> for  $^{127}\text{Xe}$  on 06/20/2018.

**Table 1. The measured  $^{37}\text{Ar}$  and  $^{127}\text{Xe}$  activities in sample aliquots from the UNESE Phase 2 injection gas, decay corrected to the injection date.**

Sample ID	Activity Concentration				
	$^{37}\text{Ar}$ [Bq/m <sup>3</sup> ]	$\pm$ [%]	$^{127}\text{Xe}$ [Bq/m <sup>3</sup> ]	$\pm$ [%]	$^{37}\text{Ar}/^{127}\text{Xe}$
Sample A	$2.76 \times 10^{13}$	2.77	$5.23 \times 10^{13}$	3.46	0.527
Sample C	$2.53 \times 10^{13}$	2.64	$4.73 \times 10^{13}$	2.82	0.534
Best Value	$2.64 \times 10^{13}$	3.83	$4.98 \times 10^{13}$	4.47	0.531

### 3.0 Initial analysis of $^{127}\text{Xe}$ in UNESE Phase 1 samples

As part of Phase 1 of UNESE, air samples were collected from a series of boreholes surrounding the Barnwell UNE after injection of  $^{37}\text{Ar}$  and  $^{127}\text{Xe}$  tracer gas. These samples were separated and counted on  $\beta$ - $\gamma$  coincidence systems similar to those used by Cooper et al. 2007.

For the initial analysis of these spectra, a triangular ROI was selected which covered all of the major features of the  $^{127}\text{Xe}$  spectrum as shown in Figure 1. Using the number of counts in the background subtracted region ( $\text{Counts}_{ROI}$ ), the concentration of  $^{127}\text{Xe}$  in  $\text{mBq}/\text{m}^3$ ,  $C$ , air can be calculated by:

$$C = \frac{\text{Counts}_{ROI}}{BR_{ROI} * \epsilon_{\beta} * \epsilon_{\gamma}} \frac{\lambda}{1 - e^{-\lambda t_c}} \frac{1}{1 - e^{-\lambda t_0}} \frac{0.087}{V_{Xe}} * 1000$$

In this equation, the values for  $V_{Xe}$ , the decay constant for  $^{127}\text{Xe}$   $\lambda$ , the count live time,  $t_c$ , and the decay time between the initial injection and analysis,  $t_0$ , are assumed to be known. However, while the efficiencies of the detector can be estimated from calibrations performed using other xenon isotopes, the branching ratio for  $\beta - \gamma$  coincidences in the ROI is unknown. For the initial analysis of the samples, a term  $\psi$  is introduced, where  $\psi = BR_{ROI} * \epsilon_{\beta} * \epsilon_{\gamma}$ . Values for  $\psi$  were calculated for both detector cells 1 ( $\psi_1 = 0.3372$ ) and 2 ( $\psi_2 = 0.3678$ ).

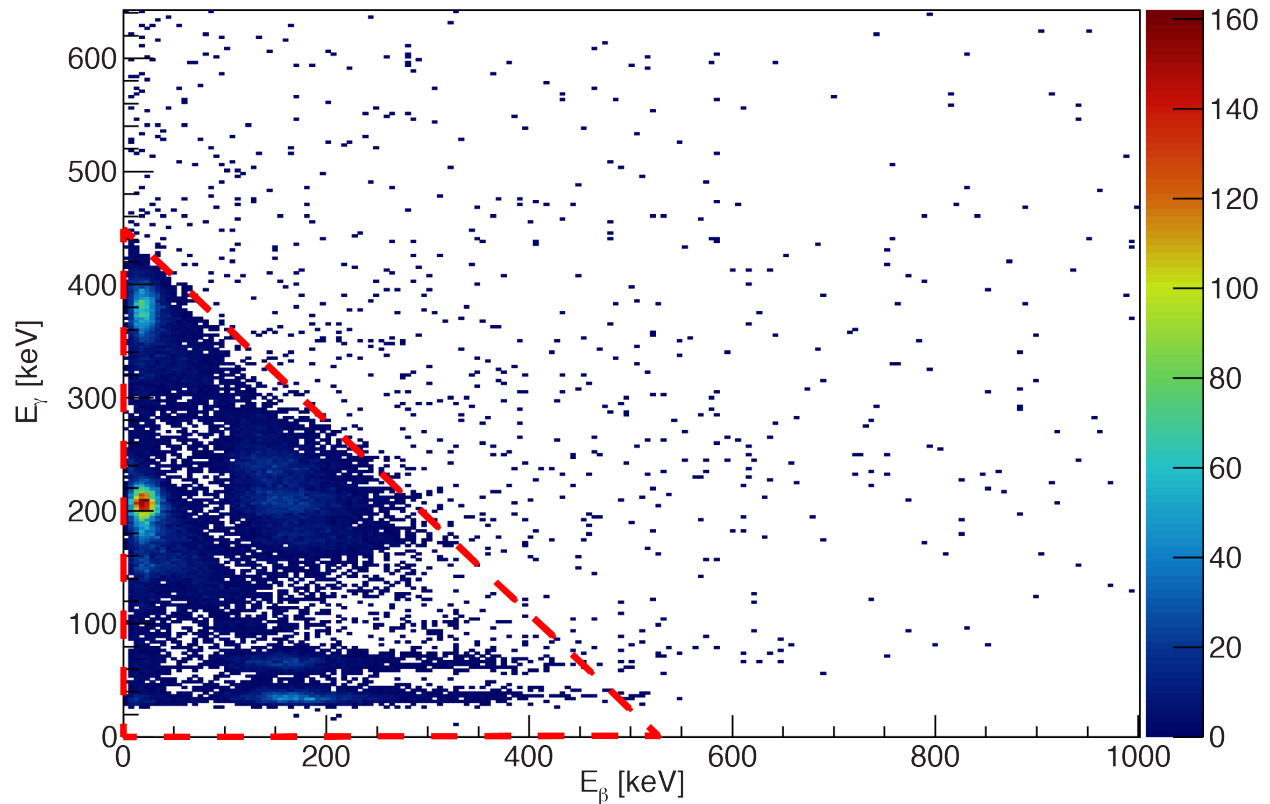


Figure 1. The  $\beta - \gamma$  coincidence spectrum of a subsurface gas sample containing  $^{127}\text{Xe}$ . The triangular ROI delineated by the red line highlights the region used in the initial analysis of the  $\beta$ - $\gamma$  spectra (C. Johnson et al. 2019).

An average of the two  $\psi$  values,  $\psi_{avg} = 0.3525$ , was chosen to represent the value for this detector setup. Using this value for  $\psi$ , the concentration in cell 1 would be calculated as  $343.8 \text{ Bq/m}^3$ , and the concentration in cell 2 would be calculated as  $76.0 \text{ Bq/m}^3$ . The error in both cases is approximately 5%.

Since a different detector system was used on the calibrated xenon source than on the subsurface gas samples, some understanding of the error introduced to the calculation is needed. Two main sources of error were considered: error in the number of counts and error in the detector efficiency values  $\varepsilon_\beta \varepsilon_\gamma$ . The uncertainty of the count is assumed to simply be the standard deviation,  $\sqrt{\text{Counts}_{ROI}}$ . The uncertainty of the value  $\psi$  was calculated by comparing the known  $\varepsilon_\gamma$  for each detector cell with the calibration detector efficiency. Since each detector cell used for the sample measurements also has its own gamma efficiency, an average of the sample detector efficiencies was used to calculate the uncertainty value.

$$\frac{\left(\frac{0.77 + 0.75 + 0.75 + 0.76}{4} - 0.56\right)^2}{\left(\frac{0.77 + 0.75 + 0.75 + 0.76}{4}\right)^2} = 0.07$$

The uncertainty introduced by the variation in gamma efficiency between detectors is thus estimated to be approximately 7%.

Once the concentration of the measured sample is calculated, the value was decay corrected to correspond with the date of injection at Barnwell. The results of using this initial analysis on a series of xenon samples collected as part of the UNESE gas transport experiment are shown in Appendix B with the associated  $^{37}\text{Ar}$  results shown in Appendix A.

## 4.0 Improved analysis of $^{127}\text{Xe}$ in UNESE Phase 1 samples

One drawback of the triangular ROI method of analysis is overestimation of low activity samples due to the presence of radon and other background sources in the sample. In an effort to improve detection of the initial arrival of xenon at the sampling boreholes, samples were reanalyzed to identify those cases where no evidence of xenon was observable. Table 2 lists those samples which were identified in the reanalysis as having minimal to no  $^{127}\text{Xe}$  signal present.

Table 2. After re-analysis of the individual spectra, the following samples were determined to contain no evidence of  $^{127}\text{Xe}$ .

Location	Sampling Depth [ft]	Sampling Date	Notes
U20Az NG-2A	436	8/22/2016	
U20Az NG-2A	436	8/25/2016	
U20Az NG-4A	459	8/25/2016	
U20Az NG-1A	385	9/1/2016	
U20Az NG-2A	436	9/1/2016	
U20Az NG-4A	459	9/8/2016	Radon
U20Az NG-1A	385	9/15/2016	Radon
U20Az NG-2A	436	9/15/2016	
U20Az NG-3A	340	9/15/2016	Radon
U20Az NG-5A	435	9/15/2016	Radon
U20Az NG-1A	385	9/28/2016	
U20Az NG-2A	436	9/28/2016	
U20Az NG-3A	340	9/28/2016	
U20Az NG-4A	459	9/28/2016	
U20Az NG-1A	385	9/29/2016	Radon
U20Az NG-2A	436	10/5/2016	
U20Az NG-4A	459	10/19/2016	
U20Az NG-1A	385	10/20/2016	Radon
U20Az NG-3A	340	10/20/2016	Radon
U20Az NG-2A	436	10/31/2016	
U20Az NG-1A	385	11/3/2016	
U20Az NG-2A	436	11/3/2016	
U20Az NG-4A	459	11/3/2016	
U20Az NG-1A	385	12/13/2016	
U20Az NG-3A	340	12/13/2016	
U20Az NG-4A	459	12/13/2016	
U20Az NG-5A	435	12/13/2016	
U20Az NG-4	284	4/12/2017	

The results in Table 2 highlight that there was a systematic error in the analysis of the samples collected early in the UNESE Phase 1 experiment that over-reported the xenon concentrations in samples with little to no activity present. This served to obscure any real arrival of  $^{127}\text{Xe}$  in the noise. As a result, previous analyses used the  $^{37}\text{Ar}$  arrivals shown in Appendix A to cross-verify arrivals of  $^{127}\text{Xe}$ .

Appendix C lists the most current  $^{127}\text{Xe}$  concentrations which account for the improved analysis described here. What immediately stands out is the likely arrival of  $^{127}\text{Xe}$  in NG-5A earlier than previously realized. In previous analyses this arrival was lost in the noise of other low to zero concentration results. With the re-analyses of those results the arrival of  $^{127}\text{Xe}$  in September 2016 becomes apparent and the slow increase in  $^{127}\text{Xe}$  also becomes visible. This is in spite of the fact that no  $^{37}\text{Ar}$  was detected in NG-5A until late October 2016 (Appendix A).

## 5.0 Progress on a future analysis method

Work was also conducted on developing a new method to quantify the  $^{127}\text{Xe}$  concentration from beta-gamma measurements. Initial method development utilized a subsample of the injection gas described in Section 2. This provided a sample with a known  $^{127}\text{Xe}$  concentration to verify the accuracy of the newly developed method. This section describes the work conducted to this point and provides a starting point for future work on analysis of the beta-gamma spectra of  $^{127}\text{Xe}$ .

### 5.1 Regions of Interest (ROI)

Prior work by Klingberg *et al.* used ROIs which took into account the  $\beta$ - $\gamma$  coincidences between the three 100-200 keV  $\gamma$  rays with the two  $\beta$  signatures, as shown in Figure 2. These three ROIs are independent of the traditional radioxenon ROIs, as shown by the red, blue, and yellow boxes. The independence allows for any interferences between  $^{127}\text{Xe}$  and the traditional radioxenons to be negated.

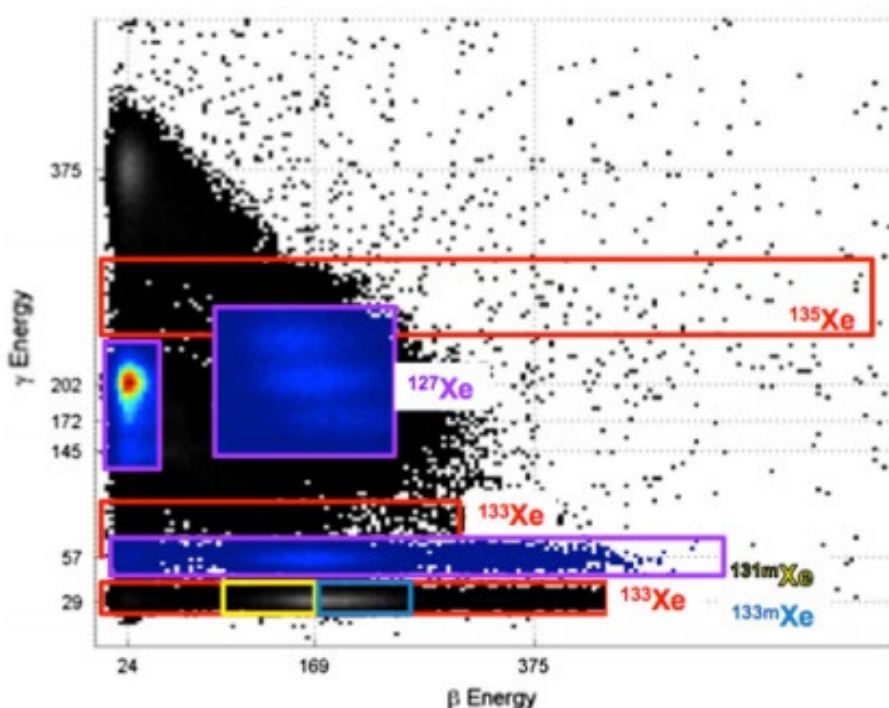


Figure 2.  $\beta$ - $\gamma$  coincidence spectrum with traditional radioxenon ROIs along with previously defined  $^{127}\text{Xe}$  ROIs in purple. (Klingberg *et al.* 2015)

During this study, similar ROIs were used as a means of calibration as opposed to means of calculating the activity and concentration, but unlike in the work by Klingberg *et al.* there was no need to avoid interference with other xenon isotopes. The ROIs utilized in this report focus on the  $\beta$ - $\gamma$  coincidences with four of the major  $^{127}\text{Xe}$   $\gamma$  rays with the two  $\beta$  signatures. Table 3 gives a relative channel number for each of the  $\gamma$ - and  $\beta$ - peak centroids, while Table 4 defines the energy ranges for the four ROIs utilized during calibration.



Table 3 – Average channels associated with the centroid of the  $\beta$  or  $\gamma$  peak in  $^{127}\text{Xe}$ .

$\beta$ Centroid		$\gamma$ Centroid	
Energy (keV)	Channel	Energy (keV)	Channel
23.6	$\sim 5 \pm 2$	28.612	$\sim 13 \pm 4$
169.691	$\sim 34 \pm 7$	57.61	$\sim 24 \pm 6$
		202.86	$\sim 76 \pm 13$
		374.991	$\sim 138 \pm 25$

Table 4 – Energy ranges for the 4 newly defined ROIs.

ROI	$\beta$ Energy Range (keV)	$\gamma$ Energy Range (keV)
1	5 (5) – 44 (11)	332 (14) – 417 (15)
2	5 (5) – 44 (11)	117 (4) – 227(7)
3	87 (24) – 252 (22)	47 (2) – 67 (2)
4	87 (24) – 252 (22)	20 (2) – 37 (2)

To add emphasis, these four defined ROIs are a means of calibration, rather than a process to extract counts. By defining calibration ROIs, it becomes apparent if the detector calibration is accurate, which becomes crucial in the next section when the method of extracting the counts is described. Figure 3 shows an example of a calibrated  $^{127}\text{Xe}$  spike with the newly defined ROIs.

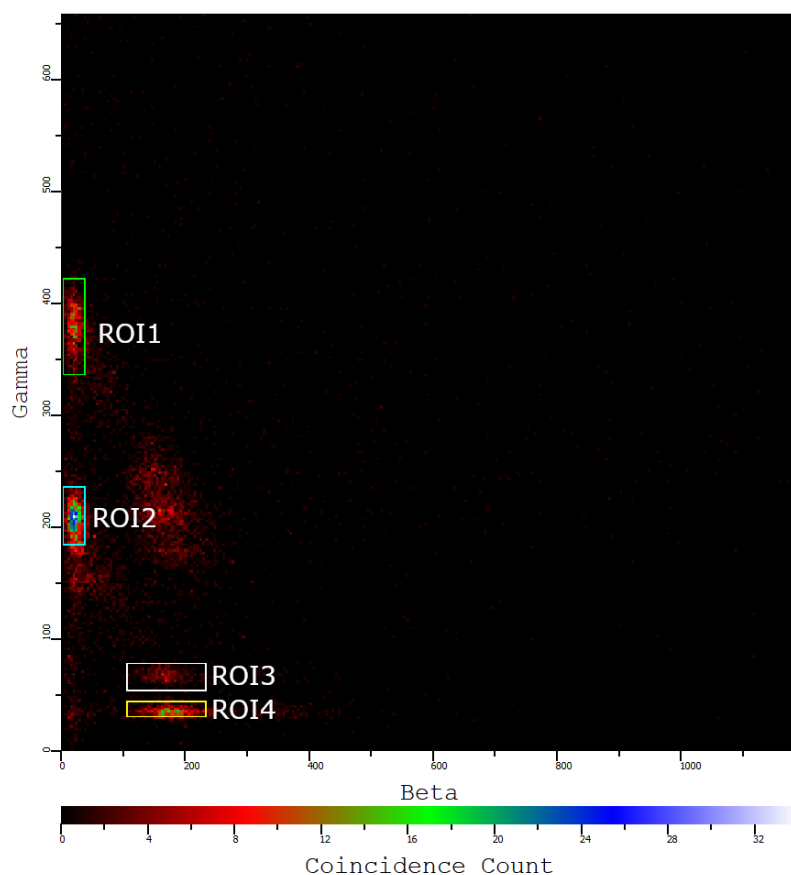


Figure 3. Newly defined ROI for  $^{127}\text{Xe}$  used for calibration purposes.

## 5.2 Extracting Counts

After the calibration is complete, counts from both the single spectra and coincidence spectra for specific associated  $^{127}\text{Xe}$   $\gamma$  and  $\beta$  peaks are extracted and used to calculate a relative efficiency. Figure 4 shows the current level scheme of the decay of  $^{127}\text{Xe}$  to  $^{127}\text{I}$ . The  $\gamma$  rays that will be specifically focused on are the 57.6- and 202.9-keV  $\gamma$  rays: both are in ROIs that do not interfere with the ROIs defined for the traditional radioxenons. The 202.9-keV  $\gamma$  ray is the strongest  $\gamma$  transition, making it straightforward to extract from the  $\gamma$  spectra. Additionally, the 57.6-keV  $\gamma$  ray is a decay transition that is not directly dependent on the  $\beta$  decay branch, allowing for clear differences in the  $\gamma$  singles spectra and the  $\gamma$  coincidence spectra.

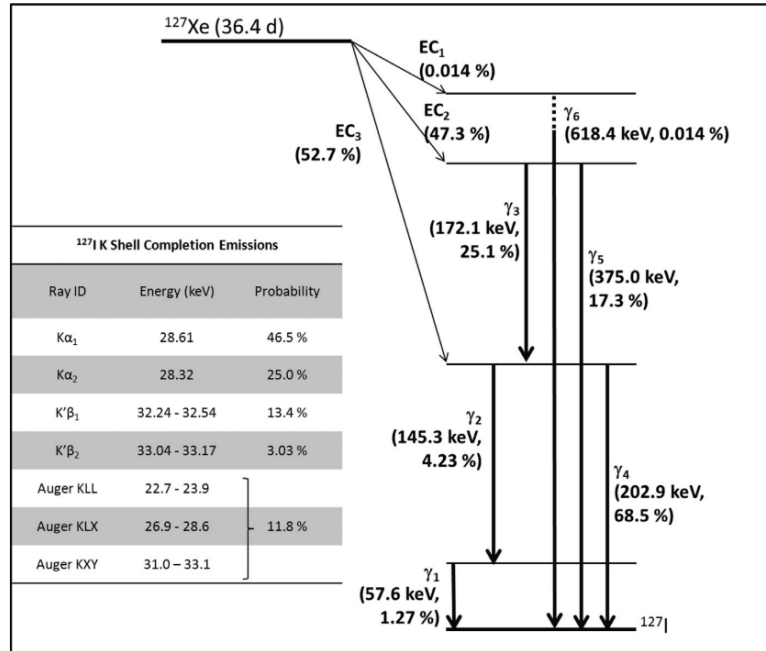


Figure 4. <sup>127</sup>Xe decay scheme with  $\gamma$  and  $\beta$  transition probabilities (Cagniant et al. 2014a).

Figure 5 and Figure 6 are the  $\beta$  and  $\gamma$  spectra, respectively, extracted from the same <sup>127</sup>Xe calibration spike as seen in the  $\beta$ - $\gamma$  coincidence spectrum in Figure 3. In both figures, the **black** curve is the single spectrum and the **red** curve is the coincidence spectrum. The peaks corresponding to the  $\gamma$  transitions in the level scheme above, along with the two  $\beta$  peaks are labelled with their respective energies. The **blue** label denotes that the peak is utilized in the relative efficiency calculations, as described below.

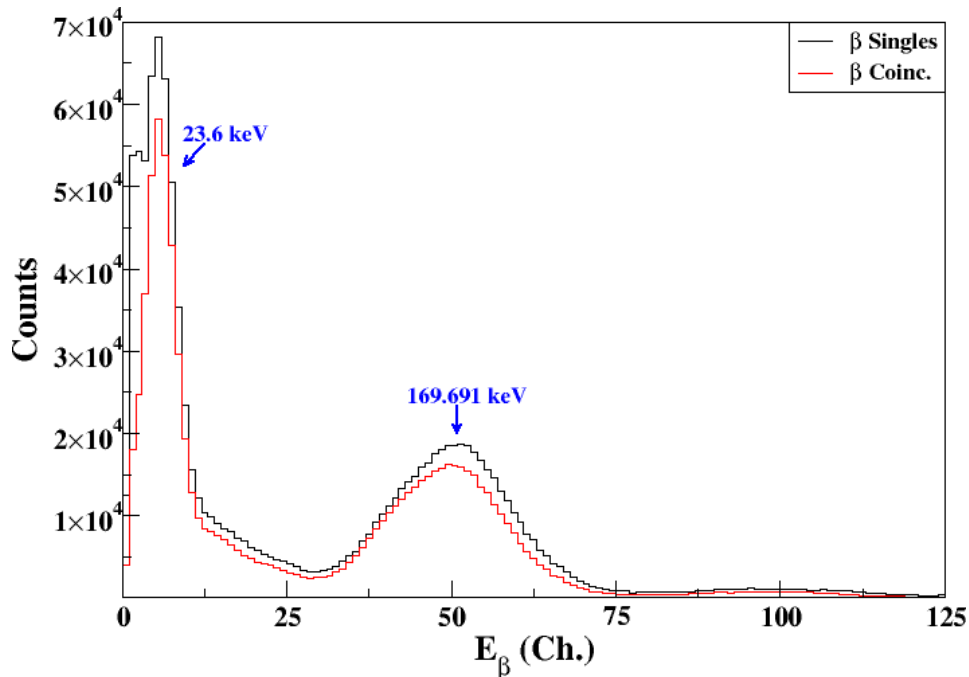


Figure 5.  $\beta$  single and coincidence spectra taken from a <sup>127</sup>Xe spike. The two  $\beta$  peaks of interest are labeled in **blue**.

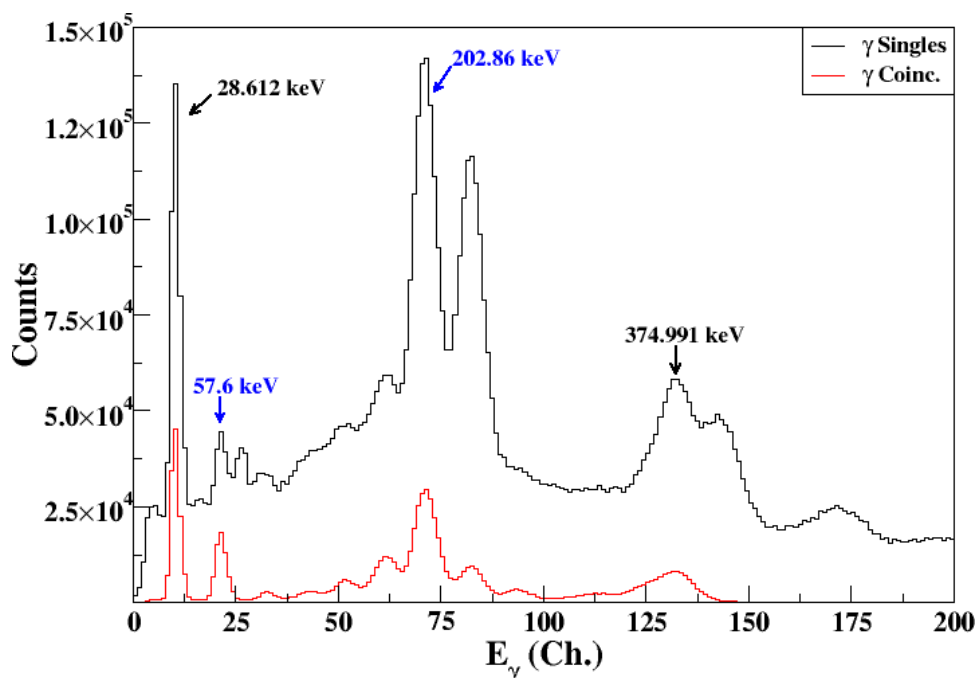


Figure 6.  $\gamma$  single and coincidence spectra taken from a  $^{127}\text{Xe}$  spike. The two  $\gamma$  peaks of interest are labeled in blue.

To extract the counts for each peak, a detector and gas background subtraction must first be made. Following the removal of any background or memory effects, the counts for each of the peaks are extracted from both the singles and coincidence spectra. Additionally, the total counts in each of the spectra (both single and coincidence for each  $\beta$  and  $\gamma$ ) must be recorded. From the total counts the activity of  $^{127}\text{Xe}$  can be calculated.

## 6.0 Conclusion

New analyses were performed on gas samples from both Phase 1 and Phase 2 of the UNESE project. The injected tracer used in Phase 2 was analyzed in proportional counters to improve the quantification of the injected  $^{37}\text{Ar}$  and  $^{127}\text{Xe}$ . This analysis found that the concentration of injected  $^{37}\text{Ar}$  was  $2.64 \times 10^{13} \pm 3.83\%$  Bq/m<sup>3</sup> while the concentration of injected  $^{127}\text{Xe}$  was  $4.98 \times 10^{13} \pm 4.47\%$  Bq/m<sup>3</sup>. These values allow for improved quantification of the total tracer injection which provides the source term for analysis of the UNESE Phase 2 noble gas migration experiment results.

The analysis of  $\beta$ - $\gamma$  spectra of Phase 1 gas samples used a triangular ROI and efficiency measurements of a  $^{127}\text{Xe}$  sample of known activity in a similar, but not identical, detector. The initial analysis was performed semi-automatically and the results are listed in Appendix B. Later examination of the results highlighted that this analysis method systematically overestimated the concentration of  $^{127}\text{Xe}$  in samples with no xenon present. A reanalysis of the Phase 1 samples identified those samples which were initially reported to have low levels of  $^{127}\text{Xe}$  when there was no actual evidence of xenon present. The reanalyzed samples are listed in Appendix C. This updated sample list reveals the likely arrival of  $^{127}\text{Xe}$  in one of the sampling boreholes (NG-5A) earlier than initially believed.

Initial work was performed to aid the development of a new analysis method for  $^{127}\text{Xe}$  from  $\beta$ - $\gamma$  spectra. The new method utilizes four targeted ROIs rather than the single broad ROI used previously. It is expected that this method would reduce the likelihood of overreported concentrations in samples with little to no  $^{127}\text{Xe}$  since less background counts would be captured. Recent observations of  $^{127}\text{Xe}$  in environmental air samples collected on a next generation beta-gamma xenon detection system highlight the need for improved analysis methods for  $^{127}\text{Xe}$  (Ely et al. 2020) and continued development of this method is an area for future work.

## 7.0 References

- Cagniant, A., G. Le Petit, B. Nadalut, P. Gross, H. Richard-Bressand, J. P. Fontaine, and G. Douysset. 2014. "On the Use of  $^{127}\text{Xe}$  Standards for the Quality Control of CTBTO Noble Gas Stations and Support Laboratories." *Applied Radiation and Isotopes* 89: 176–85. <https://doi.org/10.1016/j.apradiso.2014.02.003>.
- Cooper, Matthew W., Justin I. McIntyre, Ted W. Bowyer, April J. Carman, James C. Hayes, Tom R. Heimbigner, Charles W. Hubbard, et al. 2007. "Redesigned B-g Radi Xenon Detector." *Nuclear Instruments and Methods in Physics Research, Section A: Accelerators, Spectrometers, Detectors and Associated Equipment* 579 (1): 426–30. <https://doi.org/10.1016/j.nima.2007.04.092>.
- Ely, James H, Matthew W Cooper, James C Hayes, Justin I McIntyre, Michael F Mayer, and Mark E Panisko. 2020. "Observations of Environmental Xe-125, Xe-127, and Xe-129m." PNNL-30653.
- Gohla, H., M. Auer, Ph Cassette, R. K. Hague, M. Lechermann, and B. Nadalut. 2016. "Radi Xenon Standards Used in Laboratory Inter-Comparisons." *Applied Radiation and Isotopes* 109: 24–29. <https://doi.org/10.1016/j.apradiso.2015.11.044>.
- Johnson, C., C.E. E. Aalseth, T.R. R. Alexander, T.W. W. Bowyer, V. Chipman, A.R. R. Day, S. Drellack, et al. 2019. "Migration of Noble Gas Tracers at the Site of an Underground Nuclear Explosion at the Nevada National Security Site." *Journal of Environmental Radioactivity* 208–209 (September): 106047. <https://doi.org/10.1016/j.jenvrad.2019.106047>.
- Johnson, Christine, James Fast, Brian Milbrath, Justin Lowrey, Brad Fritz, Thomas Alexander, Michael Mayer, et al. 2020. "UNESE Phase 2: Injection and Measurement of Gaseous Tracers at U-12p Tunnel." PNNL-30202.
- Klingberg, Franziska, Steven Biegalski, Derek Haas, and Amanda Prinke. 2015. " $^{127}\text{Xe}$  Coincidence Decay Analysis in Support of CTBT Verification." *Journal of Radioanalytical & Nuclear Chemistry* 305 (1): 225–32. <https://doi.org/10.1007/s10967-014-3871-x>.
- Mace, Emily K., Craig E. Aalseth, Anthony R. Day, Eric W. Hoppe, Justin I. McIntyre, Allen Seifert, and Richard M. Williams. 2018. "Direct Low-Energy Measurement of  $^{37}\text{Ar}$  and  $^{127}\text{Xe}$  in a Radiotracer Gas Using Low-Background Proportional Counters." *Journal of Radioanalytical and Nuclear Chemistry* 318 (1): 125–29. <https://doi.org/10.1007/s10967-018-6074-z>.
- Olsen, K. B., R. R. Kirkham, V. T. Woods, D. H. Haas, J. C. Hayes, T. W. Bowyer, D. P. Mendoza, et al. 2016. "Noble Gas Migration Experiment to Support the Detection of Underground Nuclear Explosions." *Journal of Radioanalytical and Nuclear Chemistry* 307 (3): 2603–10. <https://doi.org/10.1007/s10967-015-4639-7>.

## Appendix A – UNESE Phase 1 <sup>37</sup>Ar Results

The table below lists the <sup>37</sup>Ar concentrations measured from samples collected as part of the UNESE Phase 1 Noble Gas Migration Experiment at the site of the historic Barnwell UNE. For each sample, the borehole and depth from ground surface is provided and samples are listed in order of collection date. The measured concentration of <sup>37</sup>Ar and the associated measurement uncertainty are decay corrected to the date of injection for every sample.

Borehole	Sampling Depth [ft]	Sampling Date	Ar-37	Ar-37 Unc
			Concentration [mBq/SCM]	[mBq/SCM]
U20Az NG-1A	385	8/11/2016	0.00E+00	1.51E+02
U20Az NG-2A	436	8/11/2016	0.00E+00	6.15E+01
U20Az NG-3A	340	8/11/2016	8.10E+01	9.60E+01
U20Az NG-4A	459	8/11/2016	0.00E+00	1.95E+03
U20Az NG-5A	435	8/11/2016	0.00E+00	8.27E+01
U20Az NG-2A	436	8/22/2016	3.51E+02	2.48E+02
U20Az NG-2A	436	8/25/2016	0.00E+00	9.58E+01
U20Az NG-4A	459	8/25/2016	0.00E+00	4.13E+02
U20Az NG-1A	385	9/1/2016	0.00E+00	2.59E+02
U20Az NG-2A	436	9/1/2016	0.00E+00	3.64E+01
U20Az NG-3A	340	9/1/2016	1.57E+02	9.12E+00
U20Az NG-4A	459	9/8/2016	3.15E+02	1.35E+02
U20Az NG-5A	435	9/8/2016	0.00E+00	7.04E+01
U20Az NG-1A	385	9/15/2016	0.00E+00	2.00E+01
U20Az NG-2A	436	9/15/2016	0.00E+00	8.22E+02
U20Az NG-3A	340	9/15/2016	0.00E+00	1.29E+02
U20Az NG-5A	435	9/15/2016	0.00E+00	1.77E+02
U20Az NG-3A	340	9/28/2016	0.00E+00	2.16E+02
U20Az NG-5A	435	9/28/2016	0.00E+00	1.63E+02
U20Az NG-5A	435	9/29/2016	0.00E+00	7.40E+02
U20Az NG-3A	340	10/19/2016	0.00E+00	3.20E+02
U20Az NG-5A	435	10/20/2016	6.25E+03	1.09E+03
U20Az NG-4A	459	10/31/2016	1.74E+02	6.55E+01
U20Az NG-1A	385	11/3/2016	8.92E+01	6.26E+01
U20Az NG-3A	340	11/3/2016	1.34E+03	1.10E+03
U20Az NG-5A	435	11/3/2016	1.17E+04	1.83E+03
U20Az NG-2A	436	12/13/2016	0.00E+00	1.81E+03
U20Az NG-5A	435	12/13/2016	6.22E+04	3.21E+03
U20Az NG-1A	385	12/14/2016	3.93E+05	8.45E+03
U20Az NG-2A	436	12/14/2016	0.00E+00	1.67E+04
U20Az NG-3A	340	12/14/2016	0.00E+00	1.35E+05

Borehole	Sampling Depth [ft]	Sampling Date	Ar-37	Ar-37 Unc. [mBq/SCM]
			Concentration [mBq/SCM]	
U20Az NG-5A	435	12/14/2016	9.04E+05	1.64E+04
U20Az NG-3A	340	2/22/2017	4.46E+05	2.06E+04
U20Az NG-5A	435	2/22/2017	2.66E+06	8.87E+04
U20Az NG-1A	385	2/23/2017	6.42E+05	3.96E+04
U20Az NG-1A	385	2/23/2017	2.33E+06	7.50E+04
U20Az NG-3A	340	2/23/2017	1.25E+06	4.35E+04
U20Az NG-5A	435	2/23/2017	6.37E+05	3.52E+04
U20Az NG-5A	435	2/23/2017	1.49E+05	2.00E+04
U20Az NG-4A	459	4/10/2017	1.98E+05	1.46E+05
U20Az NG-5A	157	4/10/2017	2.93E+05	1.83E+04
U20Az NG-1A	314	4/11/2017	1.00E+05	1.47E+04
U20Az NG-2A	436	4/11/2017	2.65E+06	2.38E+05
U20Az NG-3A	82	4/11/2017	4.07E+05	2.25E+04
U20Az NG-4A	459	4/11/2017	2.11E+05	1.00E+05
U20Az-GZ	1	4/11/2017	1.64E+05	1.82E+04
U20Az NG-1A	154	4/12/2017	7.22E+05	6.28E+04
U20Az NG-2A	436	4/12/2017	2.09E+06	7.18E+04
U20Az NG-5A	95	4/12/2017	1.29E+05	1.51E+04
U20Az-SOIL PT	1	4/12/2017	7.80E+04	8.15E+03
U20Az NG-6	23	4/25/2017	7.29E+05	2.72E+04
U20Az NG-6	14	4/25/2017	6.13E+05	2.98E+04
U20Az NG-6	8	4/25/2017	6.23E+05	3.49E+04
U20Az NG-7	27	4/25/2017	4.06E+05	2.69E+04
U20Az NG-7	16	4/25/2017	9.44E+03	1.36E+03
U20Az NG-7	6	4/25/2017	1.09E+04	4.10E+03
U20Az NG-5A	157	5/11/2017	6.94E+05	4.00E+04
U20Az NG-5A	435	6/6/2017	4.37E+04	4.93E+04
U20Az NG-4	720	6/8/2017	0.00E+00	3.00E+04
U20Az NG-5A	95	6/8/2017	3.21E+06	5.70E+05



## Appendix B – Initial UNESE Phase 1 <sup>127</sup>Xe Results

The table below lists the <sup>127</sup>Xe concentrations measured from samples collected as part of the UNESE Phase 1 Noble Gas Migration Experiment at the site of the historic Barnwell UNE using the analysis method detailed in Section 3.0. For each sample, the borehole and depth from ground surface is provided and samples are listed in order of collection date. The measured concentration of <sup>127</sup>Xe and the associated measurement uncertainty are decay corrected to the date of injection for every sample.

Location	Sampling Depth [ft]	Sampling Date	Xe-127	
			Concentration [mBq/m <sup>3</sup> ]	Xe-127 Unc. [mBq/m <sup>3</sup> ]
U20Az NG-2A	436	8/22/2016	438	52
U20Az NG-2A	436	8/25/2016	603	73
U20Az NG-4A	459	8/25/2016	1527	181
U20Az NG-1A	385	9/1/2016	1133	135
U20Az NG-2A	436	9/1/2016	1238	150
U20Az NG-4A	459	9/8/2016	6025	412
U20Az NG-5A	435	9/8/2016	7741	528
U20Az NG-1A	385	9/15/2016	2770	191
U20Az NG-2A	436	9/15/2016	1205	83
U20Az NG-3A	340	9/15/2016	3094	213
U20Az NG-4A	459	9/15/2016	5670	389
U20Az NG-5A	435	9/15/2016	4516	310
U20Az NG-1A	385	9/28/2016	1581	110
U20Az NG-2A	436	9/28/2016	4538	312
U20Az NG-3A	340	9/28/2016	5090	350
U20Az NG-4A	459	9/28/2016	1542	107
U20Az NG-5A	435	9/28/2016	3758	445
U20Az NG-1A	385	9/29/2016	4393	521
U20Az NG-5A	435	9/29/2016	2158	256
U20Az NG-2A	436	10/5/2016	2158	256
U20Az NG-3A	340	10/19/2016	2224	264
U20Az NG-4A	459	10/19/2016	1229	146
U20Az NG-1A	385	10/20/2016	2507	298
U20Az NG-3A	340	10/20/2016	3005	356
U20Az NG-5A	435	10/20/2016	3224	381
U20Az NG-2A	436	10/31/2016	3449	419
U20Az NG-4A	459	10/31/2016	4060	481
U20Az NG-1A	385	11/3/2016	1728	1902
U20Az NG-2A	436	11/3/2016	629	81
U20Az NG-3A	340	11/3/2016	30978	3663
U20Az NG-4A	459	11/3/2016	0	0

Location	Sampling Depth [ft]	Sampling Date	Xe-127 Concentration	Xe-127 Unc.
			[mBq/m3]	[mBq/m3]
U20Az NG-5A	435	11/3/2016	6078	732
U20Az NG-1A	385	12/13/2016	14578	1757
U20Az NG-2A	436	12/13/2016	2688	337
U20Az NG-3A	340	12/13/2016	0	0
U20Az NG-4A	459	12/13/2016	0	0
U20Az NG-5A	435	12/13/2016	2866	367
U20Az NG-1A	385	12/14/2016	85396	10089
U20Az NG-2A	436	12/14/2016	46426	3190
U20Az NG-3A	340	12/14/2016	51865	3567
U20Az NG-5A	435	12/14/2016	212586	25099
U20Az NG-3A	340	2/22/2017	262743	17899
U20Az NG-5A	435	2/22/2017	1217060	143622
U20Az NG-1A	385	2/23/2017	362597	42846
U20Az NG-1A	385	2/23/2017	966544	114077
U20Az NG-2A	436	2/23/2017	946032	111641
U20Az NG-3A	340	2/23/2017	556800	65726
U20Az NG-5A	435	2/23/2017	393065	46405
U20Az NG-5A	435	2/23/2017	150161	17811
U20Az NG-4A	459	4/10/2017	58009	6888
U20Az NG-5A	157	4/10/2017	177713	21008
U20Az NG-1A	314	4/11/2017	984670	116280
U20Az NG-2A	436	4/11/2017	934819	110327
U20Az NG-3A	82	4/11/2017	219535	25947
U20Az NG-4A	459	4/11/2017	62190	7378
U20Az-GZ	1	4/11/2017	88709	10508
U20Az BCK GRD AIR	0	4/12/2017	22979	2751
U20Az NG-1A	154	4/12/2017	398212	47037
U20Az NG-2A	436	4/12/2017	888696	104926
U20Az NG-4	284	4/12/2017	22729	2722
U20Az NG-4	1679	4/12/2017	35598	4245
U20Az NG-5A	95	4/12/2017	107457	12715
U20Az-SOIL PT	1	4/12/2017	67033	7948
U20Az NG-6	23	4/25/2017	344120	40642
U20Az NG-6	14	4/25/2017	368391	43503
U20Az NG-6	8	4/25/2017	383449	45285
U20Az NG-7	27	4/25/2017	274139	32382
U20Az NG-7	16	4/25/2017	29341	3509
U20Az NG-7	6	4/25/2017	28940	3456
U20Az NG-5A	157	5/11/2017	352127	41587

## Appendix C – Updated UNESE Phase 1 <sup>127</sup>Xe Results

The table below lists the <sup>127</sup>Xe concentrations measured from samples collected as part of the UNESE Phase 1 Noble Gas Migration Experiment at the site of the historic Barnwell UNE. These values represent the combination of the initial analysis effort described in Section 3.0 and the inspection described in Section 4.0. These values should be taken as the most current reporting of the <sup>127</sup>Xe concentrations measured for the UNESE project.

For each sample, the borehole and depth from ground surface is provided and samples are listed in order of collection date. The measured concentration of <sup>127</sup>Xe and the associated measurement uncertainty are decay corrected to the date of injection for every sample.

Location	Sampling Depth [ft]	Sampling Date	Xe-127	
			Concentration [mBq/m3]	Xe-127 Unc. [mBq/m3]
U20Az NG-2A	436	8/22/2016	0	52
U20Az NG-2A	436	8/25/2016	0	73
U20Az NG-4A	459	8/25/2016	0	181
U20Az NG-1A	385	9/1/2016	0	135
U20Az NG-2A	436	9/1/2016	0	150
U20Az NG-4A	459	9/8/2016	0	412
U20Az NG-5A	435	9/8/2016	1858	640
U20Az NG-1A	385	9/15/2016	0	191
U20Az NG-2A	436	9/15/2016	0	83
U20Az NG-3A	340	9/15/2016	0	213
U20Az NG-5A	435	9/15/2016	0	310
U20Az NG-1A	385	9/28/2016	0	110
U20Az NG-2A	436	9/28/2016	0	312
U20Az NG-3A	340	9/28/2016	0	350
U20Az NG-4A	459	9/28/2016	0	107
U20Az NG-5A	435	9/28/2016	3678	865
U20Az NG-1A	385	9/29/2016	0	521
U20Az NG-3A	340	10/19/2016	2175	343
U20Az NG-4A	459	10/19/2016	0	146
U20Az NG-1A	385	10/20/2016	0	298
U20Az NG-3A	340	10/20/2016	0	356
U20Az NG-5A	435	10/20/2016	3151	487
U20Az NG-2A	436	10/31/2016	0	419
U20Az NG-4A	459	10/31/2016	3972	498
U20Az NG-1A	385	11/3/2016	0	1902
U20Az NG-2A	436	11/3/2016	0	81
U20Az NG-3A	340	11/3/2016	30679	3636
U20Az NG-4A	459	11/3/2016	0	0
U20Az NG-5A	435	11/3/2016	6078	732
U20Az NG-1A	385	12/13/2016	0	1757

Location	Sampling Depth [ft]	Sampling Date	Xe-127 Concentration	Xe-127 Unc.
			[mBq/m3]	[mBq/m3]
U20Az NG-2A	436	12/13/2016	2688	337
U20Az NG-3A	340	12/13/2016	0	0
U20Az NG-4A	459	12/13/2016	0	0
U20Az NG-5A	435	12/13/2016	0	367
U20Az NG-1A	385	12/14/2016	85396	10089
U20Az NG-2A	436	12/14/2016	46426	3190
U20Az NG-3A	340	12/14/2016	51865	3567
U20Az NG-5A	435	12/14/2016	212586	25099
U20Az NG-3A	340	2/22/2017	262743	17899
U20Az NG-5A	435	2/22/2017	1217060	143622
U20Az NG-1A	385	2/23/2017	362597	42846
U20Az NG-1A	385	2/23/2017	1048706	102669
U20Az NG-2A	436	2/23/2017	946032	111641
U20Az NG-3A	340	2/23/2017	556800	65726
U20Az NG-5A	435	2/23/2017	393065	46405
U20Az NG-5A	435	2/23/2017	150161	17811
U20Az NG-4A	459	4/10/2017	58009	68 88
U20Az NG-5A	157	4/10/2017	177713	21008
U20Az NG-1A	314	4/11/2017	984670	116280
U20Az NG-2A	436	4/11/2017	934819	110327
U20Az NG-3A	82	4/11/2017	219535	25947
U20Az NG-4A	459	4/11/2017	62190	7378
U20Az-GZ	1	4/11/2017	88709	10508
U20Az BCK GRD AIR	0	4/12/2017	0	2751
U20Az NG-1A	154	4/12/2017	398212	47037
U20Az NG-2A	436	4/12/2017	888696	104926
U20Az NG-4	284	4/12/2017	0	2722
U20Az NG-4	1679	4/12/2017	35598	4245
U20Az NG-5A	95	4/12/2017	107457	12715
U20Az-SOIL PT	1	4/12/2017	67033	7948
U20Az NG-6	23	4/25/2017	344120	40642
U20Az NG-6	14	4/25/2017	368391	43503
U20Az NG-6	8	4/25/2017	383449	45285
U20Az NG-7	27	4/25/2017	274139	32382
U20Az NG-7	16	4/25/2017	29341	3509
U20Az NG-7	6	4/25/2017	28940	3456
U20Az NG-5A	157	5/11/2017	352127	41587

# **Pacific Northwest National Laboratory**

902 Battelle Boulevard  
P.O. Box 999  
Richland, WA 99354  
1-888-375-PNNL (7665)

***[www.pnnl.gov](http://www.pnnl.gov)***